INTERNATIONAL JOURNAL OF ADVANCE RESEARCH, IDEAS AND INNOVATIONS IN TECHNOLOGY

ISSN: 2454-132X
Impact factor: 6.078
(Volume 6, Issue 2)
Available online at: www.ijariit.com

Estimation of the land surface temperature using Landsat data 8 and 5: A comparative analysis of an industrial area from Rajasthan, India

Deepika Vashishtha
dvashishtha9990@gmail.com
Aligarh Muslim University, Aligarh, Uttar Pradesh

Seeta Meena
seetameena1323@gmail.com
University of Rajasthan, Jaipur, Rajasthan

Amit Sharma
amitbunty.vatts@gmail.com
Aligarh Muslim University, Aligarh, Uttar Pradesh

ABSTRACT

Land surface temperature (LST) is the radiative skin temperature of the land derived from solar radiation. It helps in understanding various environmental processes from local to global scale. However, rapid urbanization and industrialization are also contributing substantially to LST. This present study has been carried out to estimate Land surface temperature of an industrial area called 'Neem Ka Thana' in the eastern Rajasthan using Landsat data 8 and 5. A comparative analysis has also been presented for 1990 and 2019 to understand the magnitude and role of industrialization in increasing the temperature of the land. The LST has been estimated with respect to Normalized Difference Vegetation Index (NDVI) values derived from Red and Near Infrared bands. The Land Surface Temperature has been estimated using a step by step procedure incorporating Thermal band of Landsat 8 and 5 data for the month of May. This study also explains the shift in the area (sq. km) of temperature category over the period of 30 years and reflects negative association of LST with NDVI while positive relationship with NDBI.

Keywords— *Remote sensing, GIS, Land Surface Temperature (LST), Urbanization, Industrialization, Normalized Difference Vegetation Index (NDVI), Normalized Difference Built-up Index (NDBI).*

1. INTRODUCTION

Land Surface Temperature (LST) is a fundamental aspect of climate and biology, affecting organisms and ecosystems from local to global scales (G. Hulley and C. Coll, 2019). It plays a very significant role in understanding energy budget of the earth surface and also varying land surface process studies. It is a basic determinant of the terrestrial thermal behaviour, because it measures effective radiating temperature of the earth's surface. This quality makes LST a good indicator of energy partitioning at the land surface-atmosphere boundary and sensitive to changing surface conditions (Nemani et al., 1996; Wan et al., 2004; Lambin and Ehrlich, 1995; Mildrexler et al., 2009). Land surface, a part of the lower atmosphere is subjected to various anthropogenic activities (Dong et.al, 2019).

Global urbanization and increasing industrialization are substantially contributing to GHG emissions, eventually leading to a spike in land surface temperature. It also results in large scale changes in the world-wide climatic conditions, atmospheric equilibrium like global warming, global heat energy circulation, land use and land cover transformations etc. Modern space technology has been proved as a cornerstone in explaining and analyzing various natural and anthropogenic activities, their dynamics and ever-changing relationships. LST and emissivity for larger areas can only be obtained from the radiation leaving the surface, measured by the satellite sensors (Prasanjit Dash, 2002). Its role is indispensable for calibrating lowest and highest temperature of any particular place.

Landsat 8 carries two sensors, i.e. Operational Land Imager (OLI) and Thermal Infrared Sensor (TIRS). OLI collects data at a 30-meter spatial resolution with eight bands located in the visible and near infrared and the short-wave infrared regions of the electromagnetic spectrum and an additional panchromatic band of 15 m spatial resolution. In this paper, we have used Band 10 (Thermal band) as per the directions given by the USGS to precisely estimate LST. Landsat 5 Thematic Mapper (TM) images comprise of seven spectral bands. Their spatial resolution is 30 meters from band 1 to 7 except band 6 which is (TIR). Its spatial resolution is 120 meters. However, it is resampled to 30 meters.

2. STUDY AREA

Neem Ka Thana is an industrial town in Sikar district in the Rajasthan state of India. It is one of the nine sub divisions of this district and lies in its east. It is located at the coordinate 27.73˚N latitude and 75.77˚E longitude and it forms a part of Survey of India (SOI)

topographic sheets on 1:50000 scale (Fig. 1). This study area covers a total area of 1203 sq. Km. It is bordered by the Kotputli Tehsil towards East, Nangal Chaudhry Tehsil towards South, Khetri Tehsil towards North , Udaipurwati Tehsil towards west. Its average elevation varies from 300 to 400 metres above the mean sea level.

It is known for the rapid growth of cement, concrete and leather industries in this tehsil. There has been remarkable increment in their number in this study area, particularly after the implementation of new economic policy reforms of 1990s. It is a part of Jaipur division and is only 212 km from the national capital and 107 km from Jaipur city towards its south. It has rich deposits of various minerals like limestone, quartz, phelsphar etc. (Office of the District Statistical Officer, Sikar, 2016).

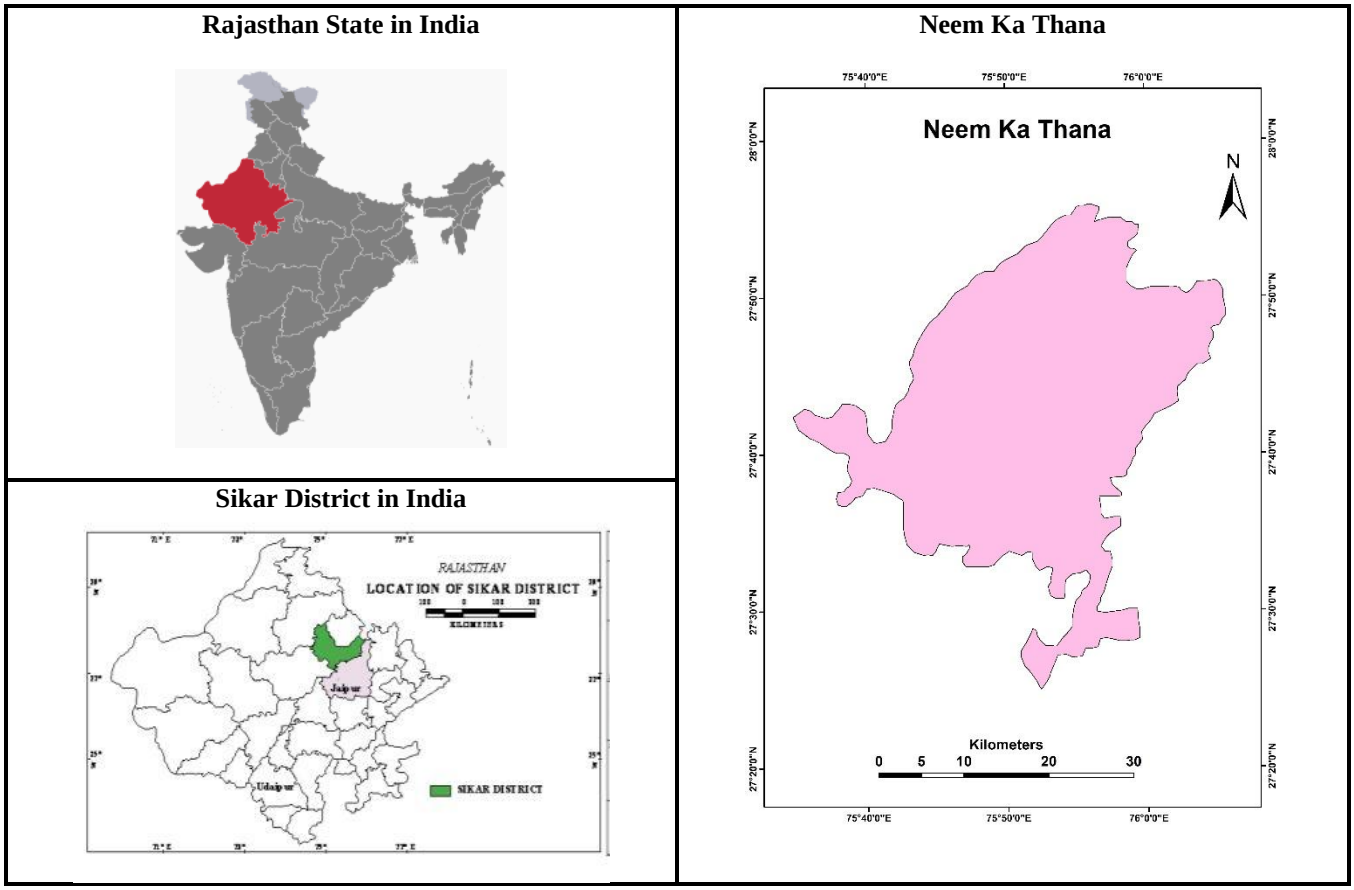

Fig. 1: Study Area

3. OBJECTIVES

This study focuses on the following objectives:

- To estimate the spatial pattern of Land Surface temperature (LST) for 1990 and 2019 using Landsat 5 and 8 data respectively of Neem Ka Thana.
- To extract NDVI and NDBI maps of the study area.
- To analyse a comparative relationship between NDVI and NDBI with LST of two respective time periods.

4. MATERIALS AND METHODS

4.1 Data Used

Landsat 8 and 5 are one of the Landsat series of NASA (National Aeronautics and Space Administration). Data pertaining to all the Landsat series can be accessed from USGS (United States Geological Survey) Earth Explorer website for research purposes. Entire earth is imaged once in 16 days using Landsat 8 and 5. In this study, TIR band 10 is used from Landsat 8 and band 6 is taken from Landsat 5 to estimate land surface temperature. Apart from this, NDVI and NDBI are also calculated using respective bands for Landsat 8 and 5. Satellite data of the study area for May 1990 and 2019 was employed to satisfy the objectives. After getting indices of NDVI and NDBI, Karl Pearson's moment of correlation coefficient technique was used to understand their relationships with LST. Landsat 8 and 5 provide various information related to the metadata of the bands such as thermal constant, rescaling factor value etc., which can be used for calculation of LST. Bands, Wavelength and resolution of Landsat 8 and Landsat 5 are given in Table 1and Table 2.

Table- 1: LANDSAT 8 OLI & TIRS

Bands	Wavelength (micrometers)	Resolution (meters)
Band 1	Ultra Blue (coastal/aerosol) 0.435	30
Band 2	Blue 0.452	30
Band 3	Green 0.533	30
Band 4	Red 0.636	30
Band 5	Near Infrared (NIR) 0.851	30
Band 6	Shortwave Infrared (SWIR) 1 1.566	30

Band 7	Shortwave Infrared (SWIR) 2 2.107	30
Band 8	Panchromatic 0.503	15
Band 9	Cirrus 1.363	30
Band 10	Thermal Infrared (TIRS) 1 10.60	30
Band 11	Thermal Infrared (TIRS) 2 11.50	30

Source: LANDSAT 8 (L8) Data Users Handbook

Following Meta data values are used for calculation
- Radiance Add Band 10 = 0.10000
- Radiance Add Band 11 = 0.10000
- Radiance Mult Band_10 = 0.0003342
- Radiance Mult Band_11 = 0.0003342
- K1 Constant band 10 = 774.8853
- K2 Constant Band 10 = 1321.0789
- K1 Constant Band 11 = 480.8883
- K2 Constant Band 11 = 1201.1442

Table 2: LANDSAT 5 OLi & TIRS

Bands	Wavelength (micrometers)	Resolution (meters)
Band 1	Blue 0.45- 0.52	30
Band 2	Green 0.52- 0.60	30
Band 3	Red 0.63 -0.69	30
Band 4	Near Infrared (NIR) 0.76-0.90	30
Band 5	Mid Infrared 1.55-1.75	30
Band 6	Thermal Infrared 10.40-12.50	30
Band 7	Mid infrared 2.08 -2.35	30

Source: LANDSAT 8 (L5) Data Users Handbook

Following Meta data values are used for calculation
- RADIANCE_MULT_BAND_6 = 5.5375E-02
- RADIANCE_ADD_BAND_6 = 1.18243
- K1_CONSTANT_BAND_6 = 607.76
- K2_CONSTANT_BAND_6 = 1260.56

4.2 Software Used
- Arc GIS 10.3
- ERDAS IMAGINE 2014 and IBM SPSS Statistics 20

4.3 Methodology

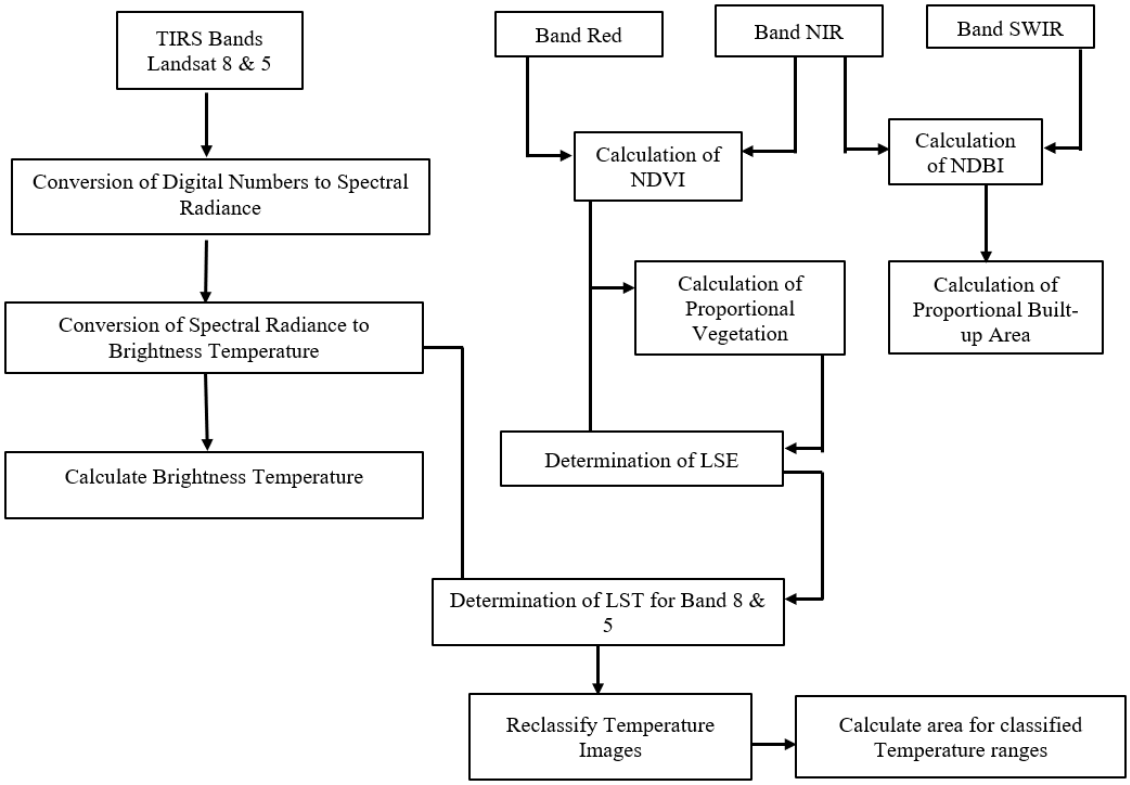

Fig. 2: Methodology, *Source: Composed by Author*

4.3.1 Process to Estimate Land Surface Temperature: There are few steps that are performed using Landsat data 8 and 5 to finally extract LST of the study area for the given time periods. These are as follows:

(i) Top of Atmosphere (TOA) Radiance: Using the radiance rescaling factor, firstly, Thermal Infra-Red Digital Numbers are converted to TOA spectral radiance with the help of following equation:

$$L\lambda = ML * Qcal + AL$$

Where
Lλ = TOA spectral radiance (Watts/ (m2*sr* μm))
ML = Radiance multiplicative Band (No.)
AL = Radiance Add Band (No.)
Qcal = Quantized and calibrated standard product pixel values (DN)

(ii) Top of Atmosphere (TOA) Brightness Temperature: Now, the spectral Radiance of each thermal band is utilized to convert the radiance into brightness temperature which can be expressed as:

$$BT = K2 / \ln (k1 / L\lambda + 1) - 272.15$$

Where:
BT = Top of Atmosphere Brightness Temperature (°C)
Lλ = TOA spectral radiance (Watts/ (m2*sr* μm))
K1 = K1 Constant Band (No.)
K2 = K2 Constant Band (No.)

(iii) Normalized Differential Vegetation Index (NDVI): NDVI is a standardized way to quantify healthy vegetation. It assesses vegetation by measuring the difference between near-infrared (which vegetation strongly reflects) and red (which vegetation absorbs). NDVI ranges between -1 to +1.

$$NDVI = (NIR – RED) / (NIR + RED)$$

Where:
RED = DN values from the Red band
NIR = DN values from the Near-Infrared band

(iv) Land Surface Emissivity (LSE): It is an inherent property of natural objects and is a significant surface parameter that is derived from the emitted radiance measured from the space. It also refers to the average emissivity of an element of the surface of the Earth calculated from NDVI values.

$$PV = [(NDVI – NDVI\ min) / (NDVI\ max + NDVI\ min)]^2$$

Where:
PV = Proportion of Vegetation
NDVI = DN values from NDVI Images
NDVI min = Minimum DN values from NDVI Image
NDVI max = Maximum DN values from NDVI Image

$$E = 0.004 * PV + 0.986$$

Where:
E = Land Surface Emissivity
PV = Proportion of Vegetation

(v) Land Surface Temperature (LST): This is the final output after calculating all these steps. It refers to the average temperature of an object of the exact surface of the Earth calculated from measured radiance.

$$LST = (BT / 1) + W * (BT / 14380) * \ln(E)$$

Where:
BT = Top of Atmospheric Brightness Temperature
W = Wavelength of emitted radiance
E = Land Surface Emissivity

5. RESULT AND DISCUSSIONS

Land Surface Temperature (LST) has been calibrated using brightness temperature and land surface emissivity (LSE). LST map for May 1990 (Fig. 3) reveals that the lowest temperature recorded was 25.40˚C, while the maximum temperature reported was 42.20˚C from the study area. This range of temperature has been divided into four categories on the basis of natural breaks. The maximum area (524 sq. km) is covered by the range of temperature i.e. 36.40˚C – 37.99˚C. However, the minimum area (51.36 sq. km) belongs to the temperature ranging between 25.40˚C to 34.43˚C. All the four temperature ranges and area covered in percentage for the month May (1990) are exhibited in Table no. 3 and graphical representation in figure 4.

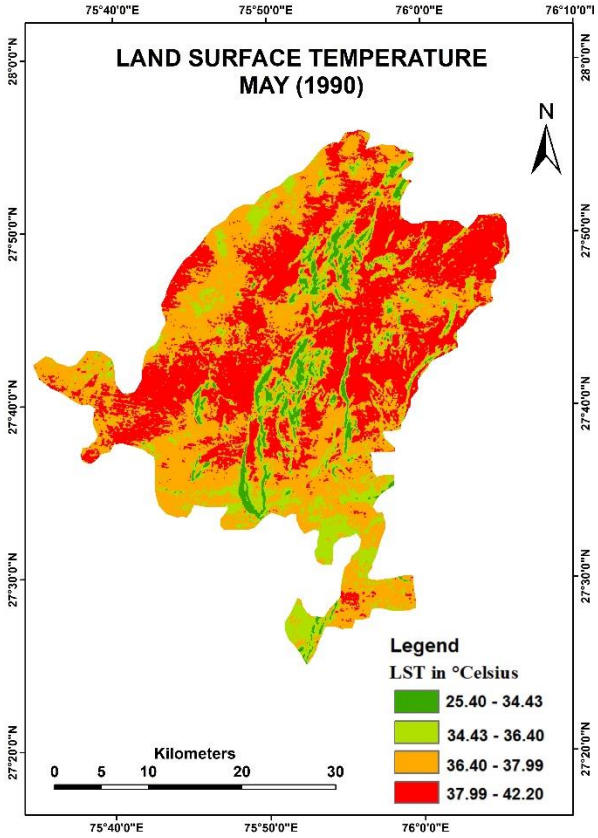

Fig. 3: Land Surface Temperature, May (1990)

Source: Composed by Author

Table 3: Area under Land Surface Temperature, May 1990

Temperature (˚C)	Area (Sq. Km)	Percentage (%)
25.40 - 34.43	51.36	4.27
34.43 - 36.40	172.99	14.38
36.40 - 37.99	524.86	43.63
37.99 - 42.20	453.53	37.7

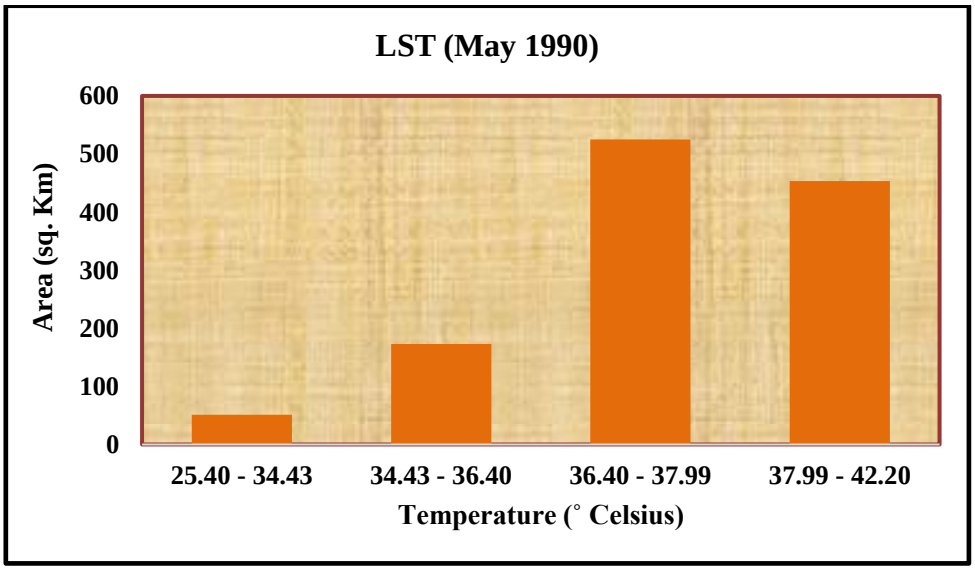

Fig. 4: Area under Land Surface Temperature, May, 1990

Source: Composed by Author

LST map for May 2019 (Fig. 5) depicts that the lowest temperature recorded was 32.02 ˚C, while the maximum temperature reported was 45.12 ˚C from the study area. Here an interesting point to note is that there has been a significant increment in the lowest temperature recorded from the Neem ka thana in 2019 than what it was reported during 1990. The temperature has shown a spike of almost 7 ˚C for the lowest category while approximately 3 ˚C increase for the highest category in 2019. This range of temperature has been divided into four categories on the basis of natural breaks. The maximum area (442.46 sq. km) is covered by the range of temperature i.e. 39.26 ˚C – 40.96 ˚C. However, the minimum area (106.94 sq. km) belongs to the temperature ranging between 32.02 ˚C to 37.05 ˚C. All the four temperature ranges and area covered in percentage for the month May (2019) are shown in Table no. 4 and graphical representation in figure 6.

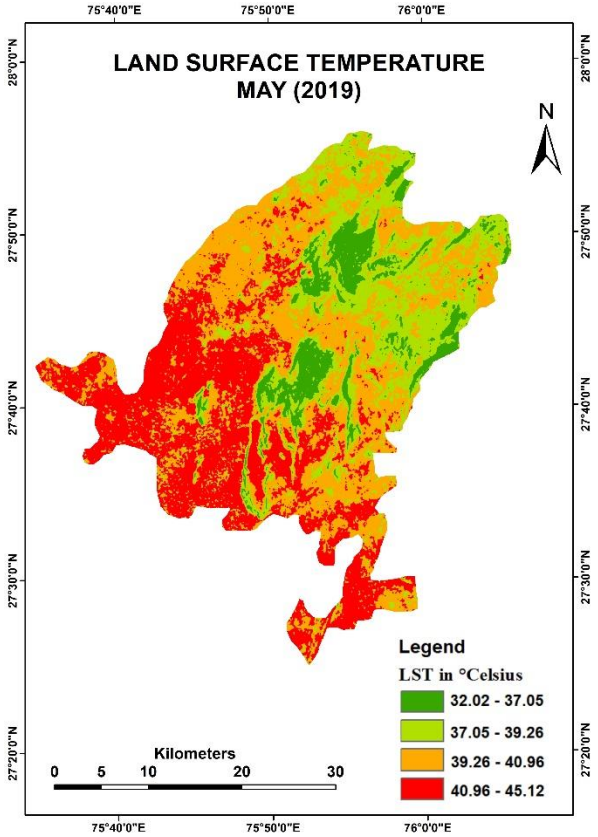

Fig. 5: Land Surface Temperature, May (2019)

Composed by Author

Table 4: Area under Land Surface Temperature, May 2019

Temperature (˚C)	Area (Sq. Km)	Percentage (%)
32.02 - 37.05	106.94	8.89
37.05 - 39.26	274.16	22.79
39.26 - 40.96	442.46	36.78
40.96 - 45.12	379.3	31.53

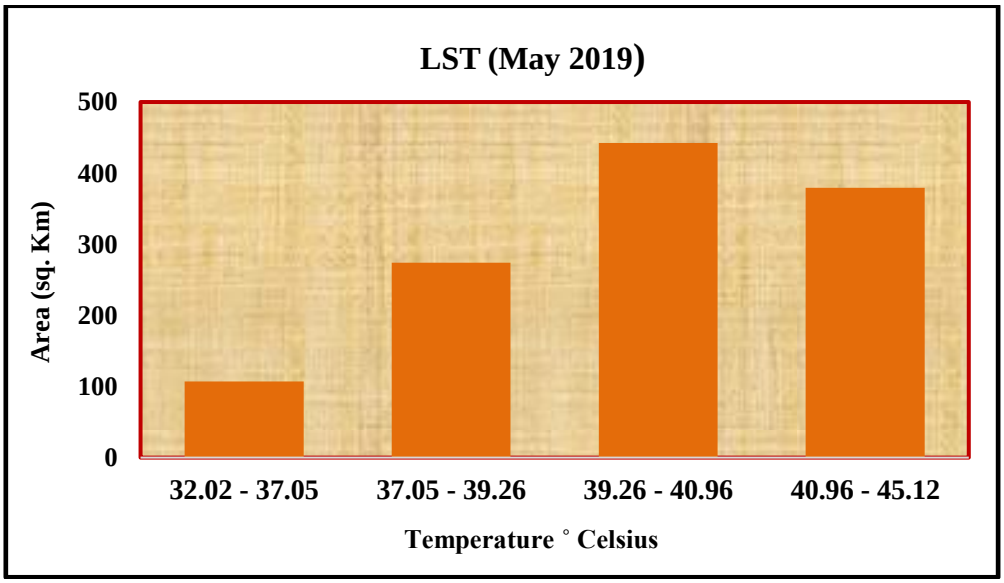

Fig. 6: Area under Land Surface Temperature, May, 2019

Source: Composed by Author

Extraction of NDVI and NDBI Maps

Normalized Difference Vegetation Index (NDVI) maps for May 1990 and 2019 have been calculated using the bands of Red and Near-Infrared from the study area. It ranges between +1 to -1.

$$NDVI = (NIR – RED) / (NIR + RED)$$

The NDVI map for the month of May (1990) shows that the NDVI values ranged between 0.470 and -0.021. Higher values of NDVI represent healthier vegetation whereas low values of NDVI indicate low or stressed vegetation or the area under water body. The result reveals high NDVI values (Figure 7).

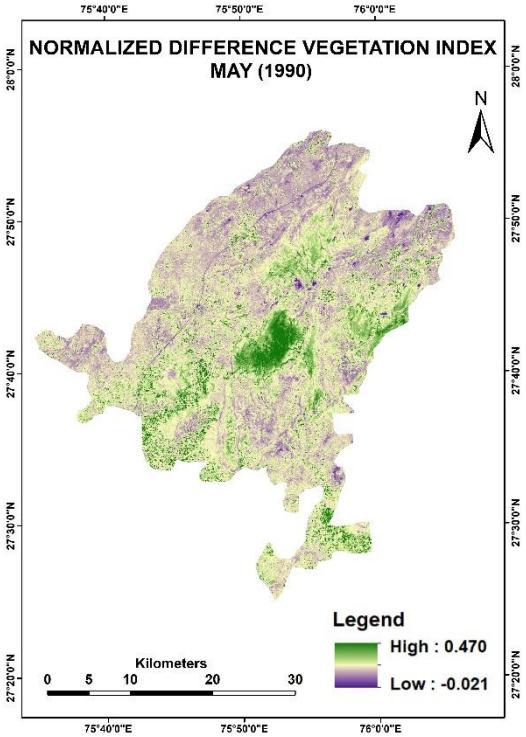

Fig. 7: NDVI, May (1990)
Composed by Author

The NDVI map for the month of May (2019) shows that the NDVI values ranged between 0.315 and -0.157. (Figure 8).

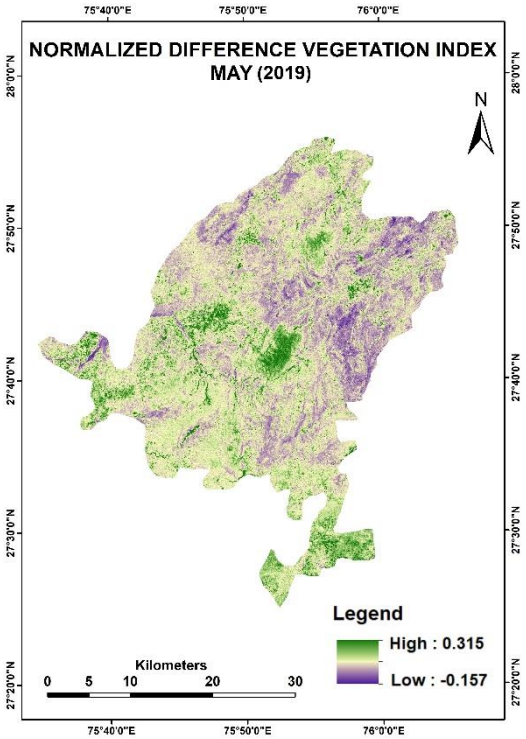

Fig. 8: NDVI, May (2019)
Source: Composed by Author

The analysis of NDVI for this year reveals that the proportion of healthier vegetation has declined than the year 1990.

Normalized Difference Built-up Index (NDBI) maps for May 1990 and 2019 have been obtained using the bands of SWIR and Near-Infrared from the study area. This index is largely employed to map built-up areas. Its values also lie between +1 to -1. Negative values of NDBI show water bodies and low urban area while positive and higher values depict dense built-up areas. This index identifies urban areas by measuring higher amount of reflectance in the shortwave-infrared (SWIR) region as compared to the near-infrared (NIR) region.

$$NDBI = (SWIR - NIR) / (SWIR + NIR)$$

The NDBI map for the month of May (1990) shows that the NDBI values ranged between 0.190 and -0.256. Higher values of NDBI represent denser built-up areas whereas low values of NDBI indicate low built-up areas or sparsely developed urban areas. (Fig. 9).

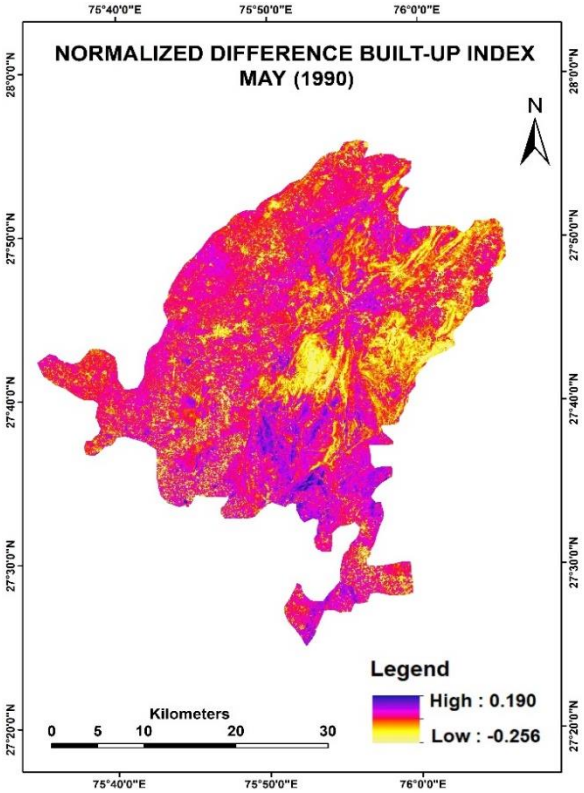

Fig. 9: NDBI, May (1990)

Source: Composed by Author

The NDBI map for the month of May (2019) shows that the NDBI values ranged between 0.381 and -0.025 (Figure 9). The findings make it very clear that there has been significant increment in the built-up area over the last thirty years. (Figure 10).

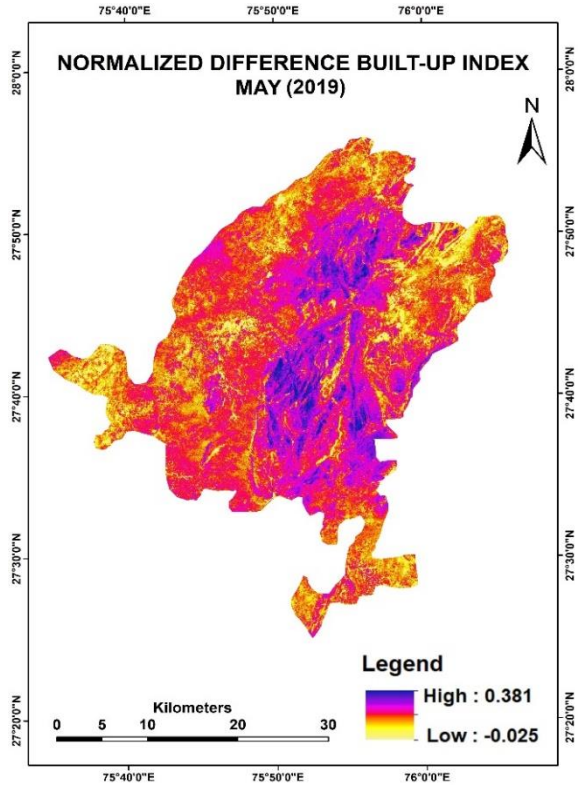

Fig. 10: NDBI, May (2019)

Source: Composed by Author

Relationship of LST with NDVI and NDBI

This paper also highlights the relationship of LST with NDVI and NDBI. For understanding this, firstly, random points were extracted as samples from the study area (Figure 11). The values pertaining to LST, NDVI and NDBI were procured using Arc Gis software and then Karl Pearson product – moment correlation coefficient was computed to assess the relationship and direction among these components. The findings of Table 5 reveal that there is a negative but significant relationship between LST and NDVI, r = -0.388, n = 120 and p = 0.05. It means that the places which reported higher temperature, they experienced lesser or low vegetation.

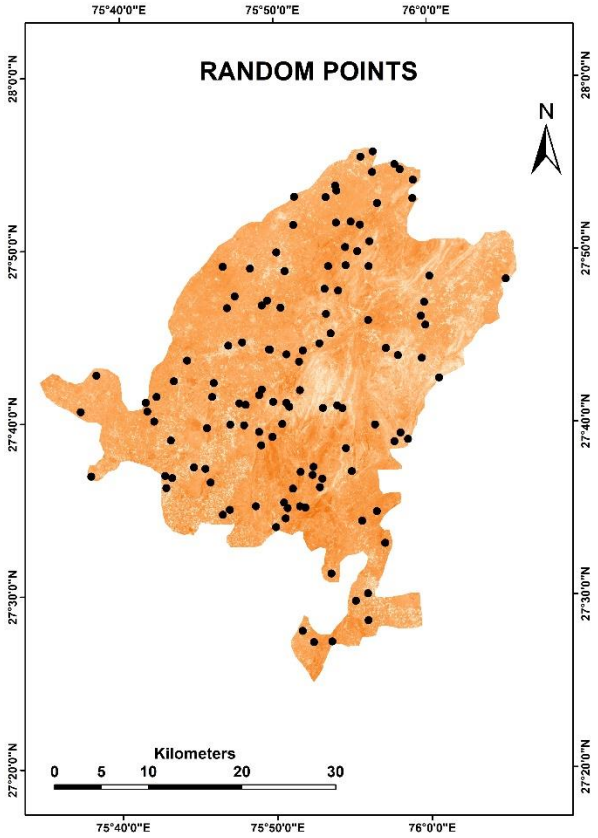

Fig. 11: Extracted Random Points
Source: Composed by Author

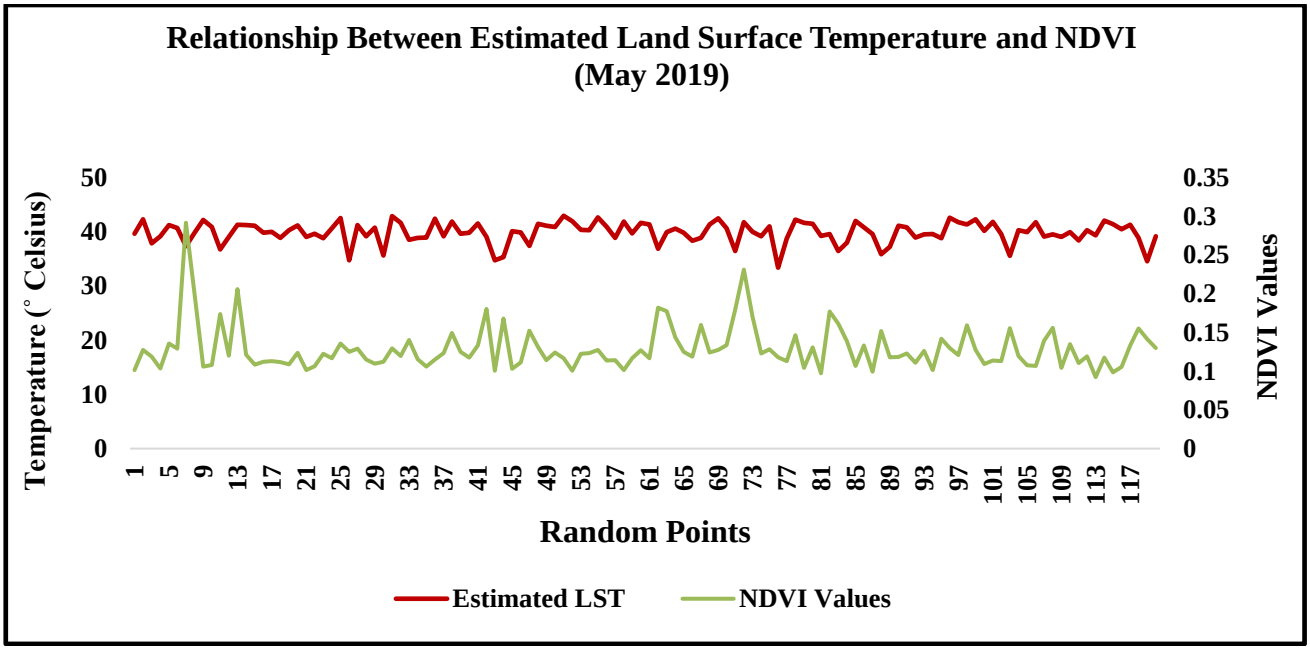

Fig. 12: Sample Points depicting relationship between LST and NDVI, May (2019)
Source: Composed by Author

Table 5: Pearson's Correlation Coefficient Matrix showing Relationship between LST & NDVI

		Land Surface Temperature (LST)	NDVI
Land Surface Temperature (LST)	Pearson Correlation	1	**-0.388***
	Sig. (2 tailed)		0.039
	N	120	120
NDVI	Pearson Correlation	**-0.388***	1
	Sig. (2 tailed)	0.039	
	N	120	120

*. Correlation is significant at the 0.05 level (2-tailed), *Source: Computed by the Author.*

However, NDBI depicts fairly strong and positive relationship with LST. Its r value being 0.505 and n = 120. It is also statistically significant at the 0.01 level (2-tailed). Thus, this analysis reveals that higher the built-up area at any place leads to increase in the land surface temperature of that area.

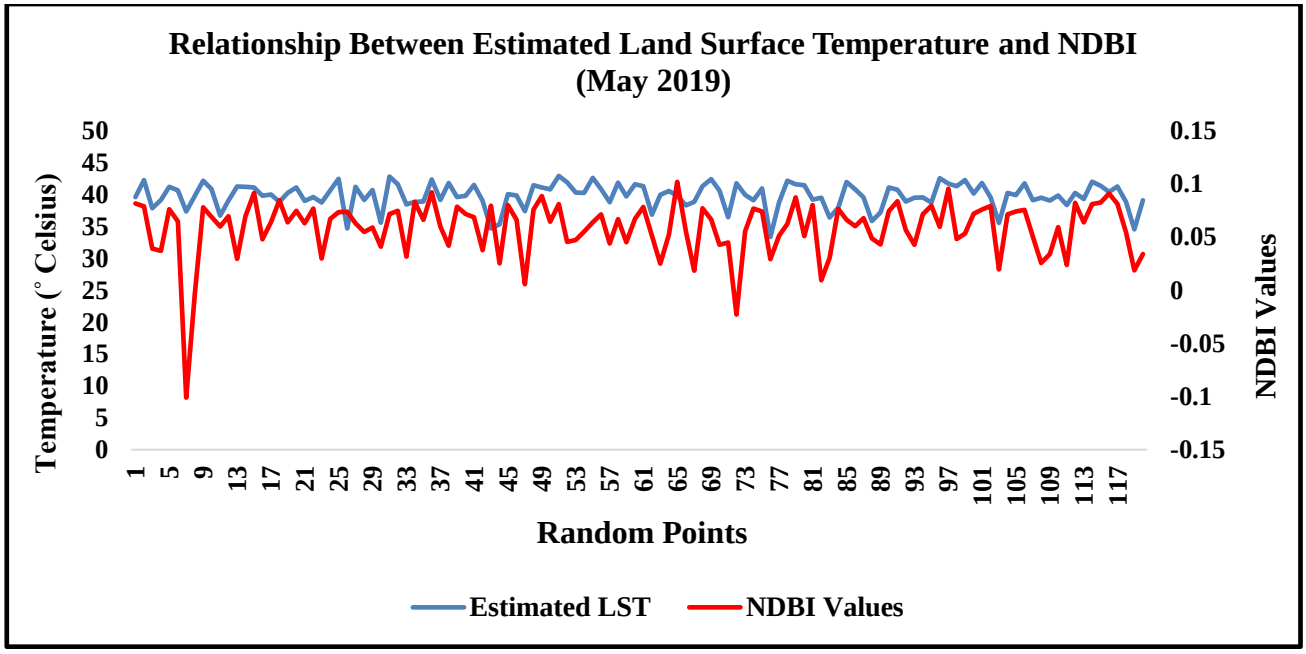

Fig. 13: Sample Points depicting relationship between LST and NDBI, May (2019)
Source: Composed by Author

Table 6: Pearson's Correlation Coefficient Matrix showing Relationship between LST & NDBI

Land Surface Temperature (LST)			**NDBI**
Land Surface Temperature (LST)	Pearson Correlation	1	**0.505****
	Sig. (2 tailed)		0.000
	N	120	120
NDBI	Pearson Correlation	**0.505****	1
	Sig. (2 tailed)	0.000	
	N	120	120

**. Correlation is significant at the 0.01 level (2-tailed), *Source: Computed by the Author.*

6. CONCLUSION

Remote sensing and GIS have emerged as the essential and crucial tools for gathering information regarding various aspects of the earth like land surface temperature, land use land cover change, atmospheric conditions and processes, global heat balance etc. These techniques are fundamental in examining the impacts of different anthropogenic activities like urbanization and industrialization. This present study is carried out for an industrial area known as Neem Ka Thana in Sikar district in the eastern Rajasthan. Two time period data i.e. 1990 and 2019 is utilized for understanding LST dynamics and its relationship with NDVI and NDBI in the study area. Landsat 8 and 5 data from USGS earth explorer is incorporated for achieving designed objectives.

The findings of this paper reveal that increasing man induced activities are largely responsible for enhancing the average temperature of the study area. Estimated LST analysis reveal that there has been a significant increment in the lowest temperature recorded from the Neem ka thana in 2019 than what it was reported during 1990. The temperature has shown a spike of almost 7˚C for the lowest category while approximately 3˚C increase for the highest category in 2019 in comparison to 1990. Normalized Difference Vegetation Index (NDVI) and Normalized Built-up Index (NDBI) were calculated. These two indices explain that the proportion of vegetation has gone down in the span of these thirty years. However, NDBI has shown increment in 2019 than 1990. Then, 120 random points were extracted as samples to understand the relationship of LST with NDVI and NDBI. This data was analysed statistically and their results demonstrate that LST is inversely associated with NDVI while it shows positive relationship with NDBI.

7. ACKNOWLEDGEMENT

The authors are highly grateful to the USGS / Landsat for providing free data and thankful to the Department of Geography, Aligarh Muslim University, Aligarh.

8. REFERENCES

[1] Anderson MC, Norman JM, Kustas WP, Houborg R, Starks PJ, Agam N, "A thermal-based remote sensing technique for routine mapping of land-surface carbon, water and energy fluxes from field to regional scales", Remote Sensing of Environment, 112:4227–4241, 2008.
[2] Candy, R. W. et al., Bulgin "The Impact of Satellite-Derived Land Surface Temperatures on Numerical Weather Prediction Analyses and Forecasts", Journal of Geophysical Research: Atmospheres, Vol 122, issue 18, pg 9783 – 9802, 27 Sept 2017.
[3] D, Anandababu, B.M Purushothaman, Babu S. Suresh, "Estimation of Land Surface Temperature using LANDSAT 8 Data", International journal of advance research, ideas and innovation in technology, Volume 4, Issue 2, ISSN: 2454-132X, 2018.
[4] David Parastatidis, Zina Mitraka, Nektrarios Chrysoulakis and Michael Abram, "Online Global Land Surface Temperature Estimation from Landsat", Remote Sensing, 9 (12), 1208, November 2017.

[5] Jiménez-Muñoz JC, Sobrino JA, Skokovi´c, D, Mattar C, Cristóbal J, "Land Surface Temperature Retrieval Methods from Landsat-8 Thermal Infrared Sensor Data", IEEE Geoscience and Remote Sensing Letters 11 (10):1840-1843, 2014.
[6] Joshi JP, Bhatt B, "Estimating Temporal Land Surface Temperature Using Remote Sensing: A Study of Vadodara Urban Area", Gujarat. International Journal of Geology Earth and Environmental Science 2(1):123-130, 2012.
[7] Katyar S.K, et al., "Impact analysis of open cast coal mines on land use/ land cover using remote sensing and GIS technique: A case study, International journal of engineering science and technology", Vol. 2 (12), pp.7171-7176, 2010.
[8] Prasanjit, Dash, Frank M. Gottsche, Folks, S, Olesen et al, "Land surface temperature and Emissivity Estimation from Passive sensor Data: Theory and Practice – Current Trends", International Journal of Remote Sensing, 23 (13): 2563, july 2002.
[9] Price JC, "Estimating surface temperatures from satellite thermal infrared data – A simple formulation for the atmospheric effect", Remote Sensing Environment, 13:353 – 361, 1983.
[10] Rajeshwari A, Mani ND, "Estimation of Land Surface Temperature of Dindigul District Using Landsat 8 Data", International Journal of Research in Engineering and Technology 3(5):122-126, 2014.
[11] S. Boussetta, A. et al., "Comparison of model land skin temperature with remotely sensed estimates and assessment of surface – atmosphere coupling", Vol. 120, Issue 23, pp. 96-111, 16 Dec, 2015.
[12] S. Narayana Reddy, et al., "Land Surface Temperature Retrieval from LANDSAT Data using Emissivity Estimation", International Journal of Engineering Research, Vol. 12, No. 20, pp. 9670-9687, 2017.
[13] Sharma, Vishwa Raj and Bist, Kamal, "Estimation of Land Surface Temperature using LANDSAT DATA: A case study of Agra city, India", Vol. 5, Issue 2, 2019.
[14] Stefania Bonafoni and Chaiyapon Keeratikasikorn, "Land Surface Temperature and Urban Density: Multiyear Modeling and Relationship Analysis Using MODIS and Landsat Data", Remote sensing, Vol. 10, 1471: doi: 10.3390/rs10091471, 14 September 2018.
[15] Ugur Avdan and Gordana Jovanovska, "Algorithm for automated mapping of the land surface temperature using LANDSAT 8 SATELLITE DATA"", Journal of sensors, Vol. 9, 2016.
[16] Xubin Zeng, et al., "Comparison of land skin temperature from a land model, remote sensing and in situ measurement", Vol. 119, Issue 6, pp. 3093-3106, 27 March, 2014.
[17] Zhao, liang, Le, Hua, Wu, Ning wang, et al., "Land surface emissivity retrieval from satellite data", International Journal of Remote sensing, 34:9 – 10, 3084-3127, 22 October, 2012.
[18] https://landsat.usgs.gov/using-usgs-landsat-8-product.

